Geophysica (2000), 36(1–2), 31–48

An Analysis of the ENSO Cycle Associated with the Equatorial Tropospheric Zonal Wind Anomalies over the Pacific Basin

Weihong Qian[1], *Haoran Hu*[1], *Yafen Zhu*[1] *and Zhongwei Yan*[2]

[1] Department of Geophysics, Peking University, Beijing 100081, China

[2] Institute of Atmospheric Physics, Beijing 100029, China

(Received: January 2000; Accepted: June 2000)

Abstract

An analysis of the El Niño/Southern Oscillation (ENSO) cycle associated with the vertically-integrated equatorial tropospheric (1000–100hPa) zonal wind anomalies (ZWA) over the Pacific Basin is made in this paper. The data sets used are the monthly US National Center of Environmental Prediction (NCEP) reanalysis wind and the NCEP monthly sea surface temperature (SST) from 1950 to 1998. The wavelet analysis of both ZWA at different regions along the equator and SST anomaly in the equatorial eastern Pacific (EEP) shows that there are various phase-lag relationships between them in the interannual and interdecadal time-scales. In the equatorial western Pacific, the phase of ZWA in most events is earlier than that of EEP SST anomaly (or El Niño event) for about 7–13 months at the interannual timescale. In the equatorial central Pacific, there is little phase-relationship between them. In the equatorial eastern Pacific, the phase of EEP SST anomaly mostly is earlier than that of ZWA for about 4–9 months while the positive ZWA leads positive SSTA about 18 months ahead. The phase of ZWA in the equatorial South America coast (ESAC) leads that of the EEP SST anomaly about 6 months in advance. In the equatorial western Pacific and ESAC, the El Niño event appears basically when the ZWA transforms from westerlies to easterlies while the La Niña event takes place in the reversed situation. The relationships are explained using a simple tropical air-sea coupled model (Gill model), which includes a positive/negative feedback scenario that seems to hold during the ENSO cycle. According to these findings, a strong El Niño is predicted for 2001–2002.

Key words: Pacific basin, equator, troposphere, wavelet transform, zonal wind, ENSO

1. Introduction

El Niño/Southern Oscillation (ENSO) is the most prominent climate variability of interannual time-scale. This phenomenon has been well recognized as a result of the ocean-atmosphere interaction in the tropics (*Philander,* 1990). ENSO was understood as an irregular low-frequency oscillation between warm (El Niño) and cold (La Niña) states with a cycle lasting several years. It receives wide attention because of its great impact on global climate and economy. The study and prediction of ENSO has been an important topic in the meteorological community since the 1980s.

As a result of the anomalous ocean-atmosphere coupling in the tropics, the low-level wind anomaly of the tropical atmosphere is an important aspect of this system. *Rasmusson and Carpenter* (1982), *Hickey* (1975), *Barnett* (1977; 1983) and others investigated the relationship between the sea surface temperature anomalies (SSTA) over equatorial eastern Pacific (EEP) and the anomaly of lower tropospheric winds (or surface wind). On the other hand, *Phillip* (1982) revealed the relationship between the upper tropospheric (200hPa) wind and ENSO events. It was found that the anomaly of zonal (or trade) wind over the tropical region usually leads the EEP SSTA about one to three months ahead.

Since the late 1980s, many efforts have been made for predicting the ENSO cycle (El Niño and La Niña) from statistical methods to dynamical models (*Zebiak and Cane*, 1987; *Ji et al*., 1996; *Latif et al*., 1994; *Barnston and Ropelewski*, 1992; *Barnett et al*., 1993; and others). However, few of those models correctly predicted the maximum of warming in early 1997 (*Trenberth*, 1998), and great discrepancy between predictions and observations has been found in the first half of 1990s (*Chen et al*, 1995; *Latif et al*., 1998). For some methods and models, once the El Niño has started, predictions can be much better. Therefore, further diagnostic analyses and theoretical studies of ENSO cycle are necessary.

Previous studies concerned in the anomalies of zonal wind in the lower or upper troposphere but present paper pays special attention to the equatorial tropospheric (1000–100hPa) temporal zonal wind anomalies (ZWA) over the equatorial Pacific Basin at different regions. The data sets used are the monthly US National Center of Environmental Prediction (NCEP) reanalysis wind and the NCEP monthly sea surface temperature (SST) from 1950 to 1998. The method used is wavelet analysis and correlation analysis for different time lags.

This paper is organized as follows: after the introduction the ZWA is examined in section 2. Wavelet transform for SSTA and ZWA at different regions is performed in section 3. The cross-lag correlation analysis is described in section 4 and a possible explanation for the relationship is addressed in section 5 using a simple dynamical model. Finally, conclusion and discussion are given in section 6.

2. ZWA at different regions over the equatorial Pacific

The data sets used are the monthly-reanalyzed winds of the NCEP with the horizontal resolution of 2.5 degrees and sea surface temperature of 2 degrees from January 1950 to December 1998. Firstly, the equatorial tropospheric ZWA in the whole equatorial zone (2.5S–2.5N) were calculated from 1000hPa to 100hPa (total 12 levels) as follows.

$$ZWA = \frac{1}{\Delta p \Delta \varphi} \int_p \int_\varphi u dp d\varphi \tag{1}$$

where, u is the local zonal wind anomaly, φ latitude from 2.5S to 2.5N crossing the equator, $1 \div \varphi = 5$, and p the pressure from 100 to 1000hPa, $\Delta p = 900$hPa. Totally 588-month ZWA time series at different longitudes are calculated relative to the climatological mean of 1950–1998. Figure 1 shows the monthly ZWA as a cross-section diagram between time (1950–1998) and longitude along the equatorial zone. The solid-line areas indicate the westerly anomalies while dashed-line areas the easterly anomalies. Obviously, westerly anomalies over large parts of the equatorial zone appeared in 1950, 1956–57, 1972, 1976, 1978–79, 1981, 1989–90 and 1997 while easterly anomalies prevailed in 1953–54, 1960–61, 1963–64 and 1973. These years with different ZWA signs concern with the exchanges of zonal wind momentum between the equatorial zone and extratropical latitudes. We pay attention to the ZWA over the Pacific Basin between 120E and 70W. In this basin, westerly anomalies dominated in early 1950, 1951–52 (west and east parts), 1956–57, 1963 (east part), 1965, 1971–72, 1975–76, 1978–79, 1981–82, 1985–86, 1992 and 1997. In some years, the westerly anomalies shift eastward from central Pacific into eastern part and in other years they move westward from the eastern coast. Remarkably, interannual variability in the ZWA series can be found. These phenomena show that there is net tropospheric convergence and divergence of zonal wind anomalies associated with the transition between westerly and easterly wind anomalies. We will examine whether the convergence/divergence or the zonal wind transition is linked to the ENSO cycle. Horizontal lines in Figure 1 indicate total 13 El Niño events or warming processes over EEP in different years. Many El Niño events associated with positive ZWA. Based on the time series of NINO3 region (5N–5S, 150W–90W) SSTA shown in Figure 2, the strong El Niño event is defined as that the SSTA should reach $+1^{o}$C persisting in 3 consecutive months and weak El Niño event larger than 0.5 ^{o}C. Under this definition using the NCEP sea surface temperature datasets, strong El Niño events from 1950 to 1998 appeared in 1957–58, 1965–66, 1968–69, 1972–73, 1976–77, 1982–83, 1986–87, 1991–92 and 1997–98. Weak El Niño events took place in 1951–52, 1953, 1963–64, 1979. Thirteen cases of warming processes have been observed in this period. The strongest process appeared in 1997–98 and the weakest one in 1979. In early 1990s, another two short-living processes taken appeared in early 1993 and late 1994. Seven El Niño events from 1950 to 1972 are the same to the cases indicated by previous studies (*Rasmusson and Carpenter*, 1982; *Philander*, 1983). Total 13 El Niño events coincide with the classification of *Trenberth* (1997), identified using NINO3 region SSTA and 0.5 °C threshold. To identify the relationship between El Niño event and ZWA, four regions over the Pacific Basin are defined in Figure 1 with double lines (120E–130E, 170E–170W, 125W–115W and 85W–75W).

Figure 2 displays the ZWA time series at four areas mentioned above and the monthly NINO3 region SSTA time series relative to the climatological mean of 1950–1996. In Figure 2, the dashed line indicates the SSTA in NINO3 region and the solid line represents the 5-month-running-mean series of ZWA. In Figure 2a, solid line

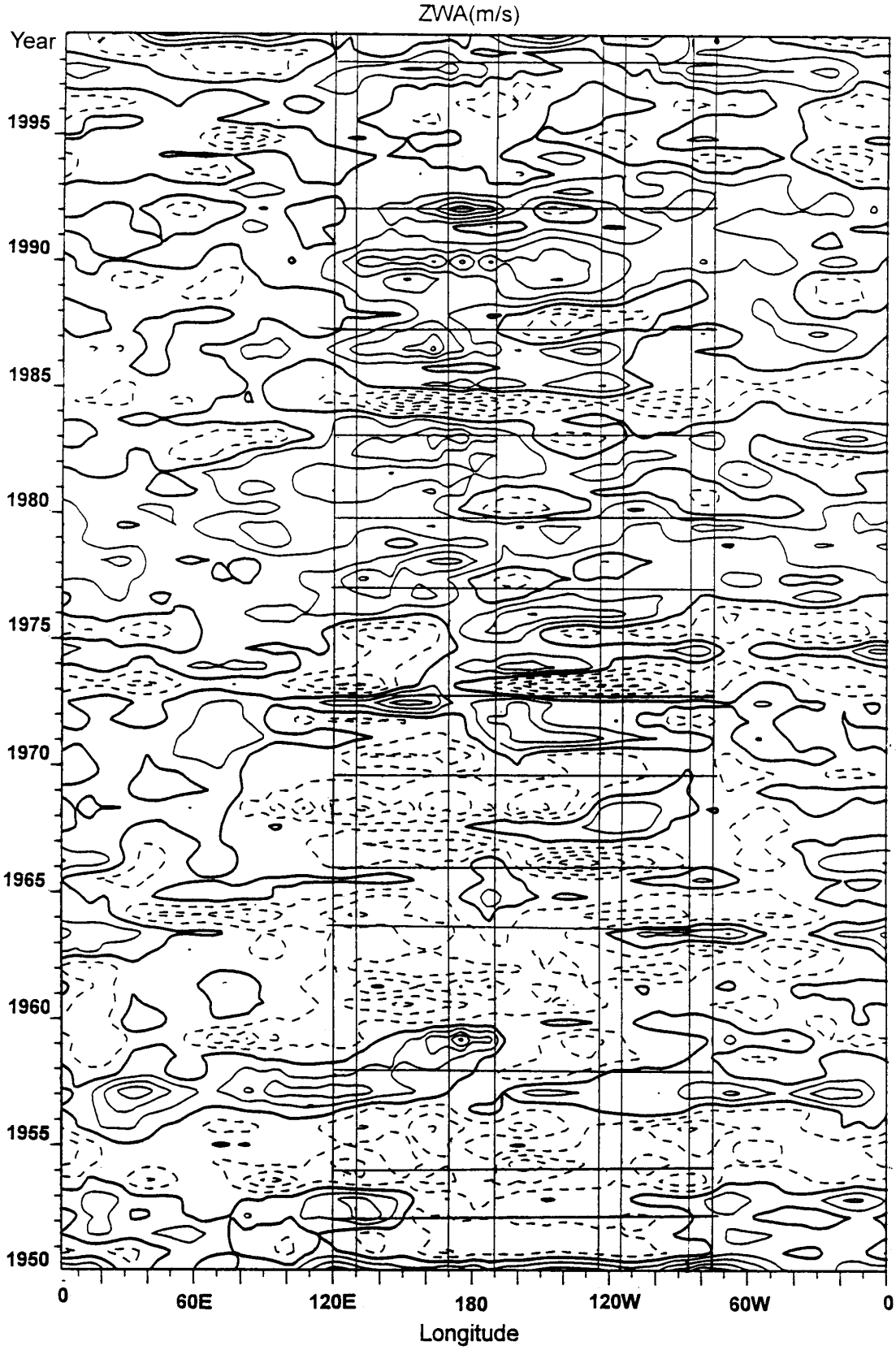

Fig. 1. Tropospheric (1000–100hPa) vertically-integrated westerly wind anomalies (solid-line areas) and easterly wind anomalies (dashed-line areas) related to climatological mean (1950–1998) along the equatorial zone (interval: 1 m/s). Horizontal lines indicate total 13 cases of El Niño appeared in different years.

presents the area-averaged ZWA at the western Pacific between 120E and 130E from 2.5S to 2.5N. In some years, positive ZWA appeared slightly earlier than positive SSTA, such as 1956–57, 1964–65, 1971–72, 1975–76, 1981–82, 1986–87, 1991, and 1996–97. In the early 1990s, two short-living warming processes accompanied two fluctuations of positive ZWA. Also, negative ZWA appeared earlier than negative SSTA for several cases, such as 1953–54, 1963–64, 1966, 1972–73, 1984, 1995 and 1998. From Figure 2a, an obvious interdecadal change for ZWA and SSTA appeared in mid 1970s. Before mid 1970s, negative ZWA and La Niña events were dominant but after that time positive ZWA and strong El Niño events were prevailing. Many investigators, such as *Wang* (1995) and *Qian et al* (1999) have noted this interdecadal change and its transition in mid 1970s. This interdecadal variation exists not only in global SSTA (*Zhu et al.* 1999) but also in tropospheric circulation. Figure 2b displays the SSTA and ZWA at the central Pacific between 170E and 170E from 2.5S to 2.5N. In this region, no statistically significant cross-lag relationship between the two time series can be found because they were sometimes opposite and sometimes synchronous in phase-variation. An interesting phase-relationship can be found in Figure 2c that negative ZWA averaged between 125W and 115W from 2.5S to 2.5N occur usually slightly later than positive SSTA in phase-variation while positive ZWA lead positive SSTA about 1~2 years ahead. If removing the interdecadal trend of ZWA, the relationship of interannual variability between ZWA and SSTA will become further clear. This relationship in eastern Pacific is different from that in the western Pacific. Opposite phase-variations for El Niño events related to ZWA occurred in 1951–52, 1953, 1957–58, 1963–64, 1965–66, 1968–69, 1972–73, 1982–83, 1987 and 1997. Another fascinating relation can be seen in Figure 2d, i.e., the ZWA averaged between 85W and 75W from 2.5S to 2.5N leads SSTA for a quarter cycle in phase-relationship not only for El Niño events but also for La Niña events in the equatorial South America coast (ESAC). For the ENSO events in 1951–52, 1957–58, 1963–64, 1965–66, 1968–69, 1972–73, 1982–83, 1986–87, 1991–92 and 1997–98, the variations of ZWA led that of SSTA 4–9 months ahead.

These relationships mentioned above are consistent with previous data analyses (*Rasmusson and Carpenter*, 1982; *Wang*, 1995) and model results (*Zebiak*, 1986; *Zebiak and Cane*, 1987) in some aspects. Based on the composite analysis of six warm episodes (1951, 1953, 1957, 1965, 1969 and 1972) using surface marine observations, *Rasmusson and Carpenter* (1982) documented a phase-relationship between central Pacific SSTA and westerly anomalies. They concluded that during October-November prior to El Niño, the equatorial easterly anomalies in the western Pacific are replaced by westerly anomalies and this change coincides with the appearance of positive SSTA in the vicinity of the equator near the dateline. This relationship is clearly seen from Figure 2a if we consider the interdecadal variation of ZWA and bring down (up) the multiple-year mean of ZWA with horizontal solid-line in the period of 1950–1975 (1976–1998). Before 1975, seven warm episodes were observed and five cases satisfied

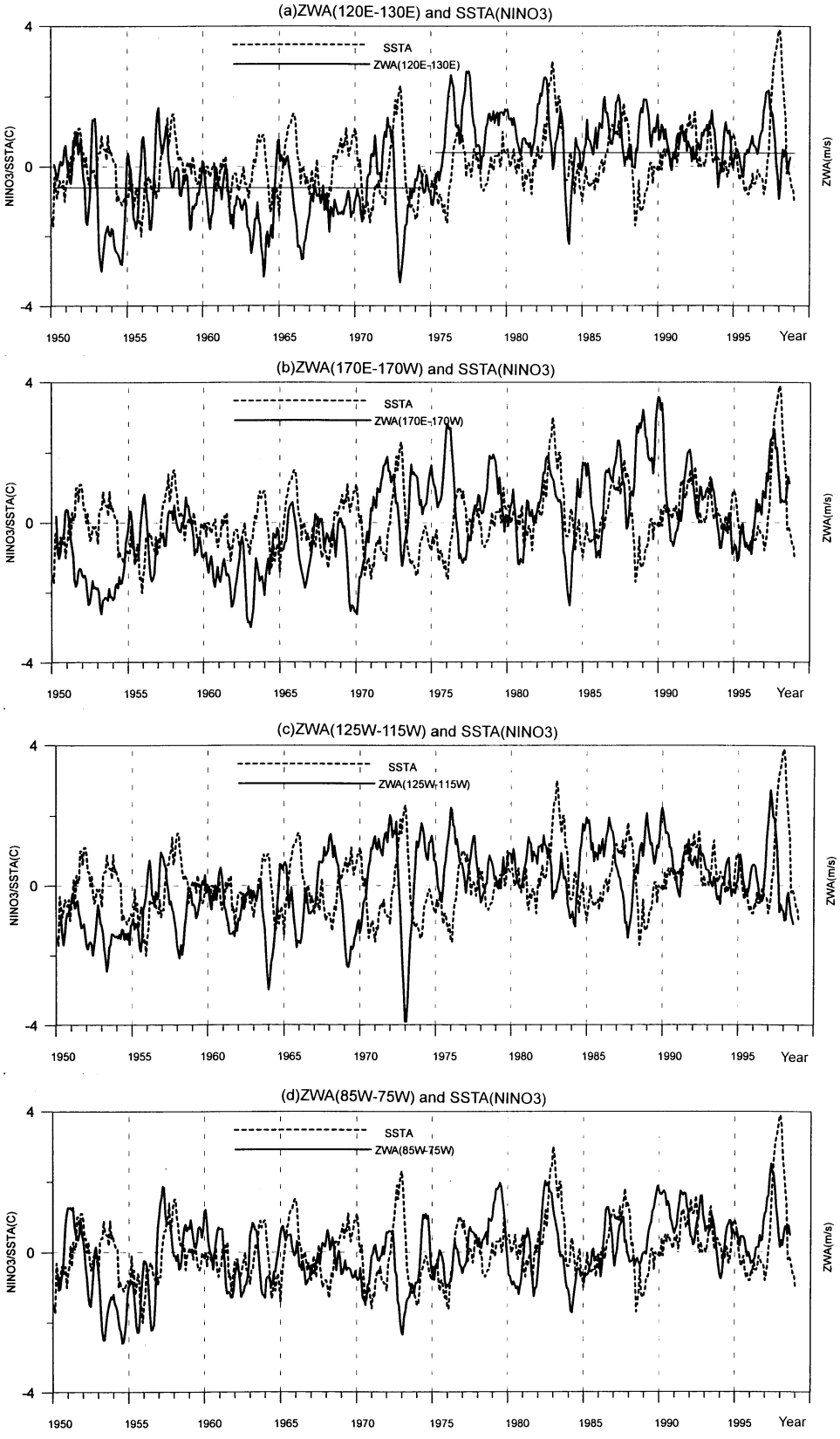

Fig. 2. Time series between NINO3 region (5N–5S, 150W–90W) SSTA (unit: ^{o}C) and ZWA (unit: m/s) of 5-month-running mean at equatorial (a) western Pacific (2.5N–2.5S, 120E–130E), (b) central Pacific (2.5N–2.5S, 170E–170W), (c) eastern Pacific (2.5N–2.5S, 125W–115W) and (d) the equatorial South America coast (2.5N–2.5S, 85W–75W). Solid horizontal lines in (a) denote the interdecadal change for ZWA series.

this relation in 1951, 1953, 1957, 1965, 1972 except 1963 and 1968–69. After 1975, eight warming processes (1976, 1979, 1982, 1986, 1991, 1993, 1994 and 1997) followed the westerly anomalies in the equatorial western Pacific except the westerly anomaly in 1988/89 without warm episode. Some cases in 1957, 1965, 1972 and 1976 were consistent with those analyzed by *Rasmusson and Carpenter* (1982) but the interdecadal transition in 1975 is a new puzzle. In the transition phase (preceding mature phase one season) of El Niño event, the westerly anomalies in the equatorial western Pacific are rather strong but there is little easterly anomaly in the equatorial eastern Pacific (*Rasmusson and Carpenter*, 1982). During mature phase, the convergence of strong meridional winds appears in the central equatorial Pacific but in equatorial western and eastern Pacific there are remarkable easterly anomalies. The surface easterly anomalies for the mature El Niño not only appeared in cases before 1975 but also in cases of 1982–83,1986–87 and 1991–92 (*Wang*, 1995). After the mature phase, easterly anomalies in the equatorial eastern Pacific were also simulated in model (*Zebiak*, 1986) even stronger than observations (*Zebiak and Cane*, 1987).

Using the wind dataset, the zonal mean ZWA (figure omitted) along the equatorial zone and subtropical latitudes were also calculated from 1950 to 1998. Relationships between ZWA along different latitudes and NINO3 region SSTA indicate that El Niño event appears when positive ZWA along the equatorial zone turns to negative one and the positive maximum of ZWA at subtropical latitudes occur in the mature phase of El Niño event. This relationship between ZWA and NINO3 region SSTA is perfectly consistent with the result of the zonal mean relative angular momentum of atmosphere which was calculated by *Dickey et al.* (1992) based on US National Meteorological Center (NMC) wind analysis during 1976–1989 for levels between 1000 and 100hPa.

Description above made a comparison of present analysis with previous works applying sea level winds and NMC winds. This comparison implies that vertically-integrated wind fields agree with the previous analyses and provide an advantage in examining the angular momentum exchanges between the equatorial zone and subtropical latitudes for a long period. Objectively, SSTA does not act only on the sea level wind but also drive the whole layer atmosphere at least tropospheric air. Different phase-relationships at western and eastern Pacific, which can not well be identified applying only surface winds, will be examined using a simple dynamical model. Following analysis first focuses on the zonal wind anomalies over different regions in the equatorial Pacific related to the ENSO cycle.

3. Wavelet transform of ZWA and SSTA

As shown in Figure 2, there is a statistical relationship between ZWA and SSTA at different regions along the equator. This relationship may be related to the multiple time-space-scale sea-air interactions. Wavelet transform method (*Lau and Weng*, 1995) can be performed to extract the interannual and interdecadal time-scale information contained within these two time series. Figure 3 shows the coefficients of wavelet trans-

forms with time-scales ranging from 2 to 150 months for the NINO3 region SSTA and ZWA at 120–130E between 2.5S to 2.5N. Figure 3(a) is the time coefficient of SSTA wavelet transform with different time scales from January 1951 to June 1998. Relatively large amplitude and regular high frequency can be found in the interannual time scales from 50-month to 80-month. Solid lines indicate positive SSTA while dashed lines, negative. Relatively strong and relatively weak El Niño events can be clearly identified from this figure. All El Niño events appeared in 1951–52, 1953, 1957–58, 1963, 1965–66, 1968–69, 1972–73, 1976–77, 1982–83, 1986–87, 1991–92 and 1997–98. A relatively weak warming appeared in 1979–80. Early in 1990s, three warming events in the 50-month time scale can be noted while in 80-month time scale only one. The same situation also happened in the period of 1951–1954. Major La Niña events occurred in 1955–56, 1967, 1970, 1974–75, 1984–85, 1988–89 and 1995–96. Decadal changes also exist in the time series of SSTA. Before 1977, La Niña events were stronger than El Niño events while relatively strong El Niño events have appeared after 1977. On the 120-month time scale, positive SSTA appeared in late 1950s~1960s, late 1970s~mid 1980s and since early 1990s.

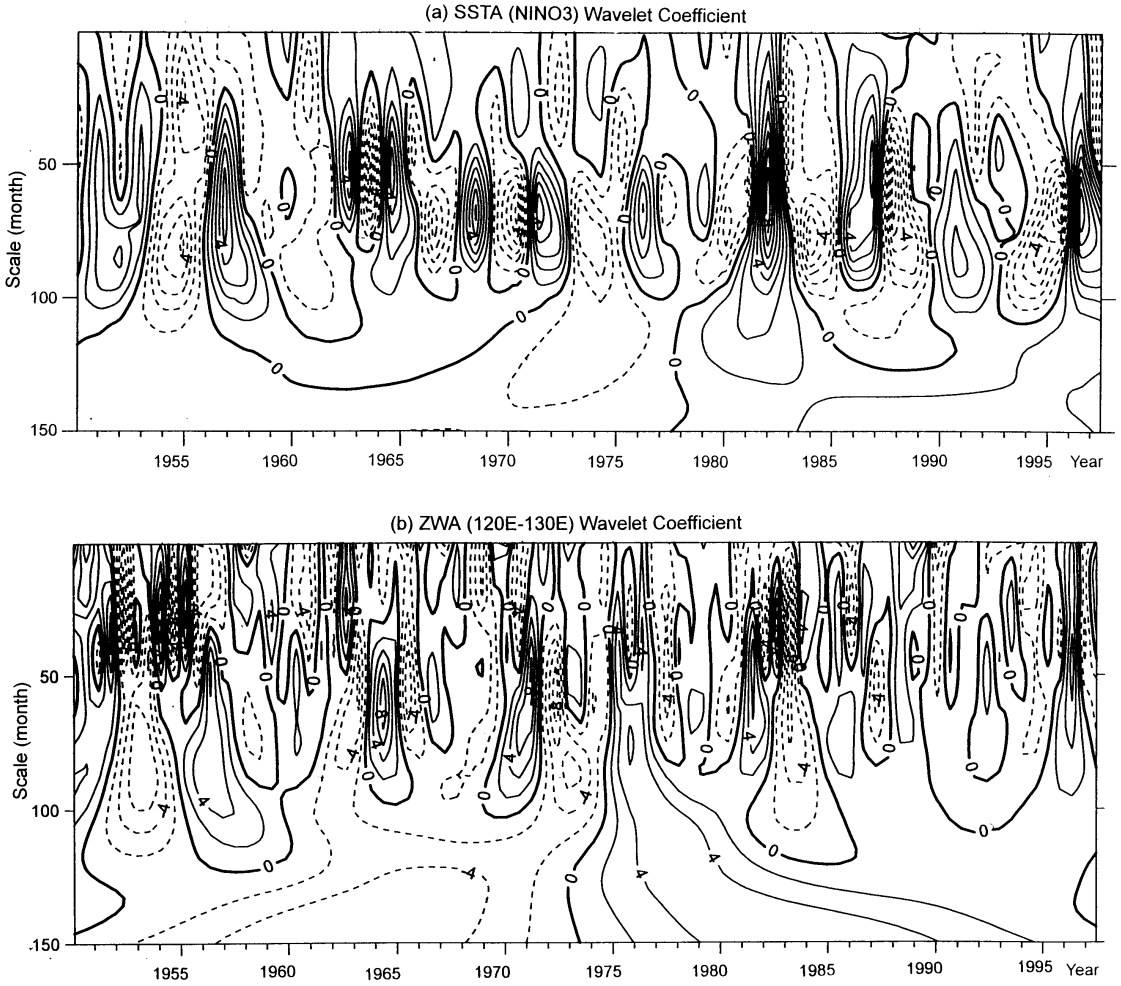

Fig. 3. Coefficients of wavelet transform with time-scale ranging from 2 to 150 months for (a) NINO3 region SSTA and (b) ZWA at the equatorial western Pacific (2.5N–2.5S, 120E–130E).

Figure 3b shows the time coefficient of ZWA wavelet transform at the region between 120E and 130E for different time scales from January 1951 to June 1998. In this figure, relatively large amplitude and high frequency dominate from several months to 100-month in time scale. Solid lines indicate positive wavelet coefficient of ZWA while dashed lines, negative. Since late 1970s, the cases of positive ZWA in 1975–76, 1979, 1982, 1985–86, 1989–90, 1993, 1994, 1996–97 were basically consistent with or preceding El Niño events, shown in Figure 3a. Also before the mid 1970s, positive ZWA in 1951, 1952, 1956–57, 1961–62, 1964–65, 1967–68 and 1970–72 were preceding those warming processes. In the interdecadal time scale (130-month) the ZWA transforms from negative into positive since mid 1970s, earlier than the transition of NINO3 region SSTA.

The time coefficients of ZWA wavelet transform at the regions over 125W–115W and 85W–75W show that obvious interannual and interdecadal variability also exist in these series (figures omitted).

4. Correlation analysis

The relationship between the NINO3 region SSTA and ZWA at different regions has been briefly touched upon in section 3. To determine at which time scale the phase-relationship holds well or more consistently, this section will display the results of cross time-lag correlation between different time-scale components with the time lag from –24 to 24 months. Figure 4 shows the time-lag correlation between SSTA and ZWA at the region of 120E–130E in the western Pacific. Pronounced positive correlation (coefficient as high as 0.6) appears at 60–90-month time-scale with a 7–13-month leading of ZWA to SSTA (Fig. 4a). If taking correlation coefficient 0.5 or –0.5 as the threshold of significant for total 13 cycles, the positive ZWA over the equatorial western Pacific leads positive SSTA in the EEP about 5–15 months ahead at 70–80-month timescale. In the interdecadal time scale, the phase-difference gradually becomes longer. Figures 4(b) and (c) show the components of wavelet transform between ZWA and SSTA at 70-month and 110-month time-scales, respectively. It could be seen that the positive ZWA in most events leads positive SSTA in advance of 7–13 months at 70-month time scale. In this time scale, strong El Niño events with the coefficient more than 4 have 8 cases (1957–58, 1965–66, 1968–69, 1972–73, 1976–77, 1982–83, 1986–87 and 1997–98) from 1951 to 1998. Total those 8 cases with ZWA preceding positive SSTA about 5–14 months can be found in this period. At the 110-month time scale, two positive SSTA processes and three negative SSTA processes are basically later than that of ZWA at phase-variations. As two time series shown in Figure 2b, no significant relationship between NINO3 region SSTA and ZWA at central Pacific can be found so the component coefficient of wavelet transform at this place is not displayed.

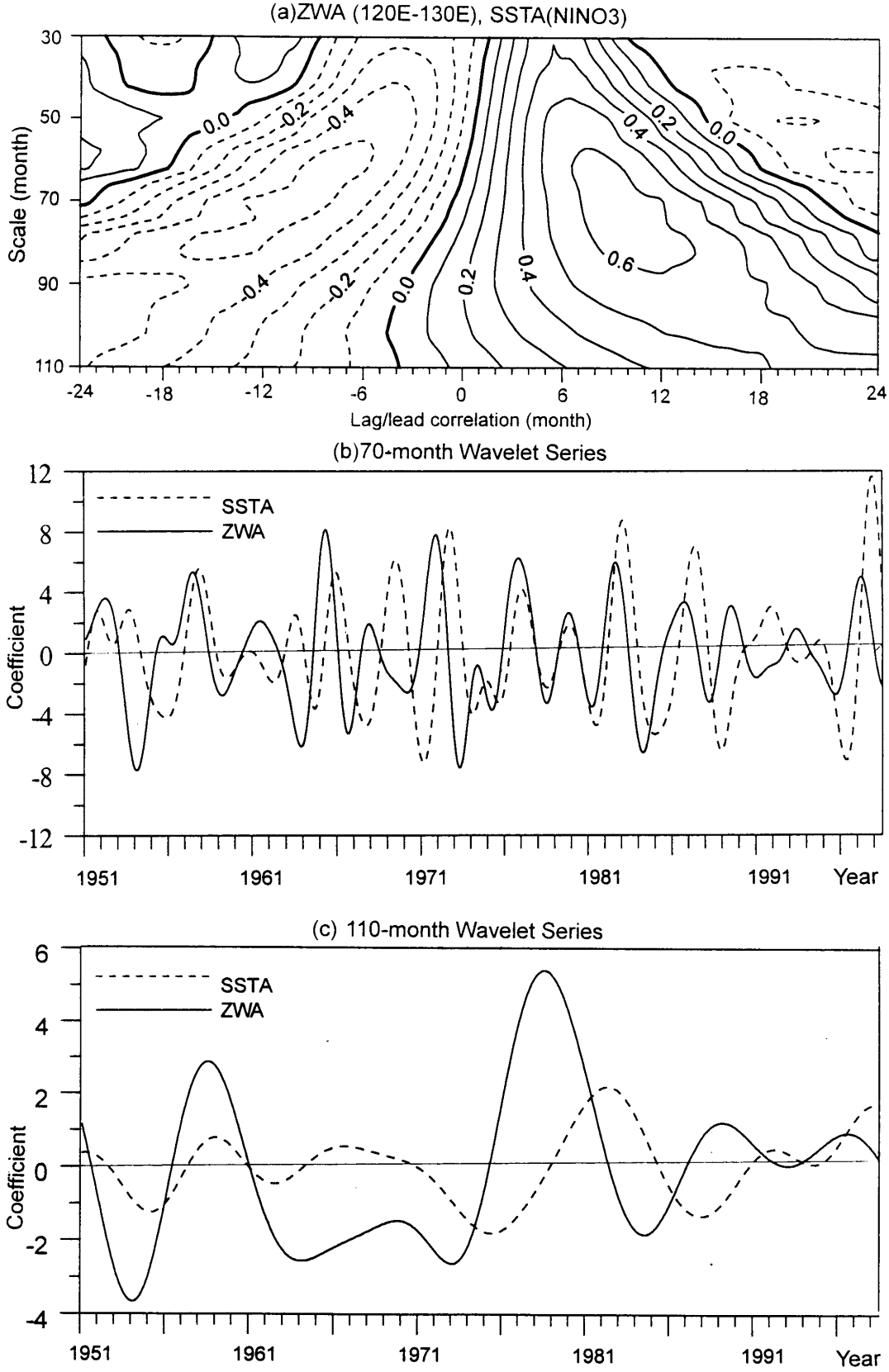

Fig. 4. (a) Time-lag correlation between NINO3 region SSTA and ZWA at the region of 120E–130E between 2.5S and 2.5N in the equatorial western Pacific, and component series of ZWA and SSTA at (b) 70-month and (c) 110-month time-scales.

Figure 5 displays the time-lag correlation between NINO3 region SSTA and ZWA at the region of 125W–115W in the eastern Pacific. Pronounced negative correlation (coefficient as high as –0.7) appears at 70–80-month time-scale and positive correlation (coefficient as high as 0.7) at 80-month time scale (Figure 5a). The relationship depicted in Figure 5a implies that the positive SSTA leads easterly (trade wind) anomaly at eastern Pacific about 1–12 months ahead with significant threshold larger than 0.5 while the positive ZWA leads positive SSTA about 18 months ahead at 80-month timescale. To see this relationship more clearly, Figure 5b and c show their time series of wavelet components at 70-month and 80-month time scales respectively. The phases of both ZWA and SSTA are opposite to each other basically but the positive peak of SSTA for major El Niño events mostly leads that of negative ZWA about 4–9 months ahead. The relationship in Figure 5b is better than that shown in Figure 4b. In Figure 5c, the result is more exciting in that the variations of both ZWA and SSTA are rather regular. Noted in Figure 5c that several active periods of El Niño cycle and ZWA from 1951 to 1998 should be divided according to their frequency variations. The first active period began before 1960 with a relatively lower frequency cycle of about 5 years. The second active period existed between 1965 and 1975 with a relatively higher frequency cycle, of about 4 years. The third one ranged from 1981 to 1989 with a 4.5-year cycle. The fourth active period started in 1996 with the first cycle of El Niño. During each active period, there are 3~4 ZWA and El Niño cycles persisting sequentially for about one decade. According to the above, there should be at least three El Niño cycles between 1996 and 2005. In the 21st century, the first strong El Niño event can be expected to happen in 2001/02 and the second in 2005. Between any two active periods, there is a quiet period, or period of frequency modulation, for about 5 years. Therefore, the difficulty of predicting El Niño emerged during the periods of frequency modulation, such as early 1960s, mid 1970s and early 1990s. In the quiet period, ocean and atmosphere are uncoupled. This result can explain why the relatively lower predictability was found in the mid 1970s and the early 1990s (*Chen et al.*, 1995).

Finally, we pay attention to the relationship between NINO3 region SSTA and ZWA at the region 85W–75W shown in Figure 6. Obviously, the positive correlation (coefficient as high as 0.6) appears at 60–100-month time-scales with the 4–9-month leading of ZWA to SSTA (Figure 6a). It means that the positive ZWA at the South American coast leads SSTA rising in the EEP about 4–9 months ahead, usually. The lag-time with high correlation coefficient gradually becomes longer when the time scale rises from 70 months to 110 months. Figure 6b and c show the components of wavelet transform between ZWA and SSTA at 70-month and 110-month time-scales. The figure suggests that the positive ZWA lead positive SSTA about 2–10 months ahead at 70-month time scale. At 110-month time scale, the phase-lag relationship is also clearly seen since 1970s. Relationships shown in Figure 4 and Figure 6 indicate that the El Niño (La Niña) event appears when ZWA at western Pacific and equatorial South

American coast turn its phase from westerly (easterly) to easterly (westerly) anomalies for major ENSO cycle from interannual to interdecadal time scales.

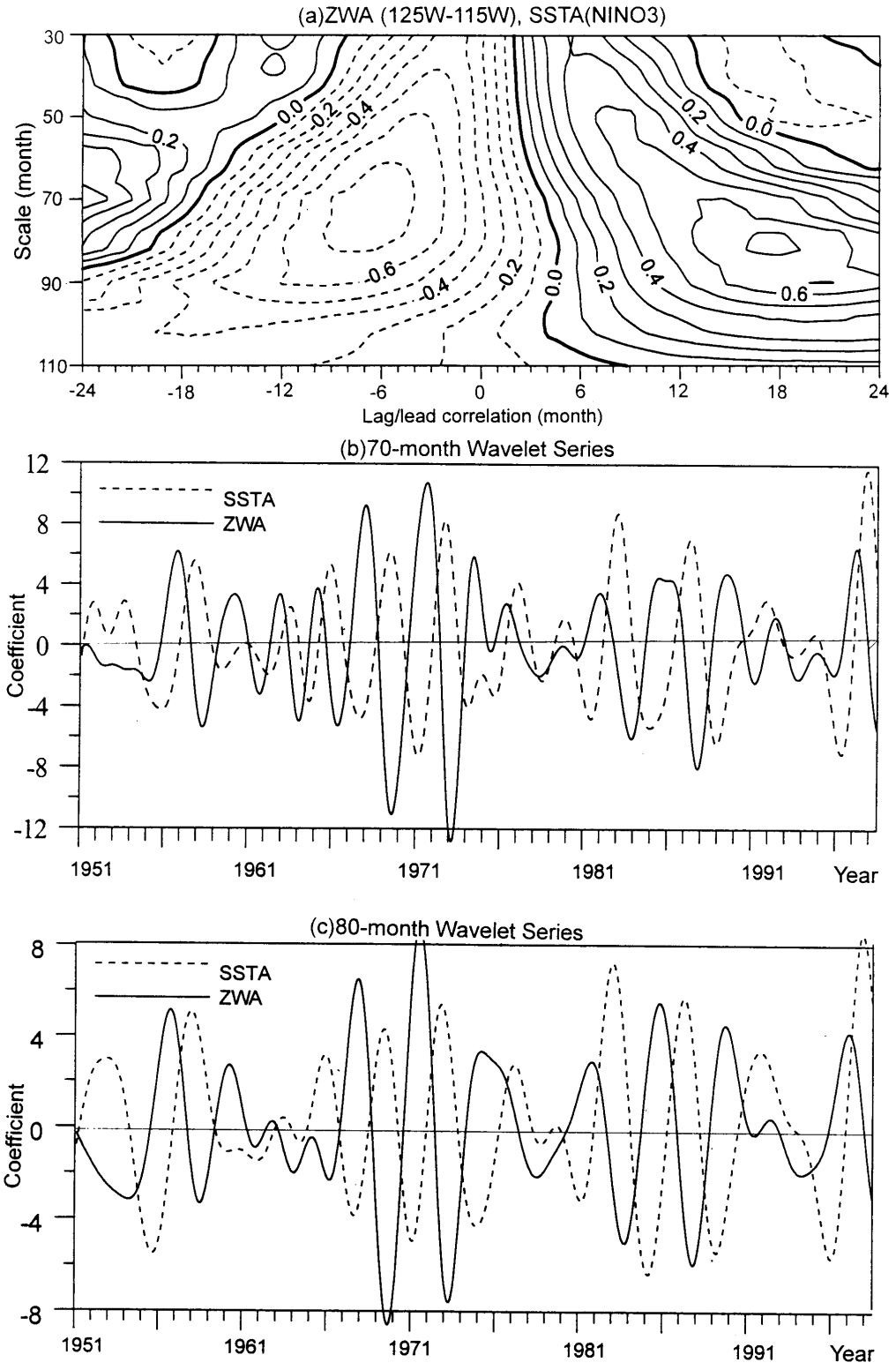

Fig. 5. Same as in Figure 4 but for ZWA at the region of (a) 125W–115W, and component series of ZWA and SSTA at (b) 70-month and (c) 80-month time-scales.

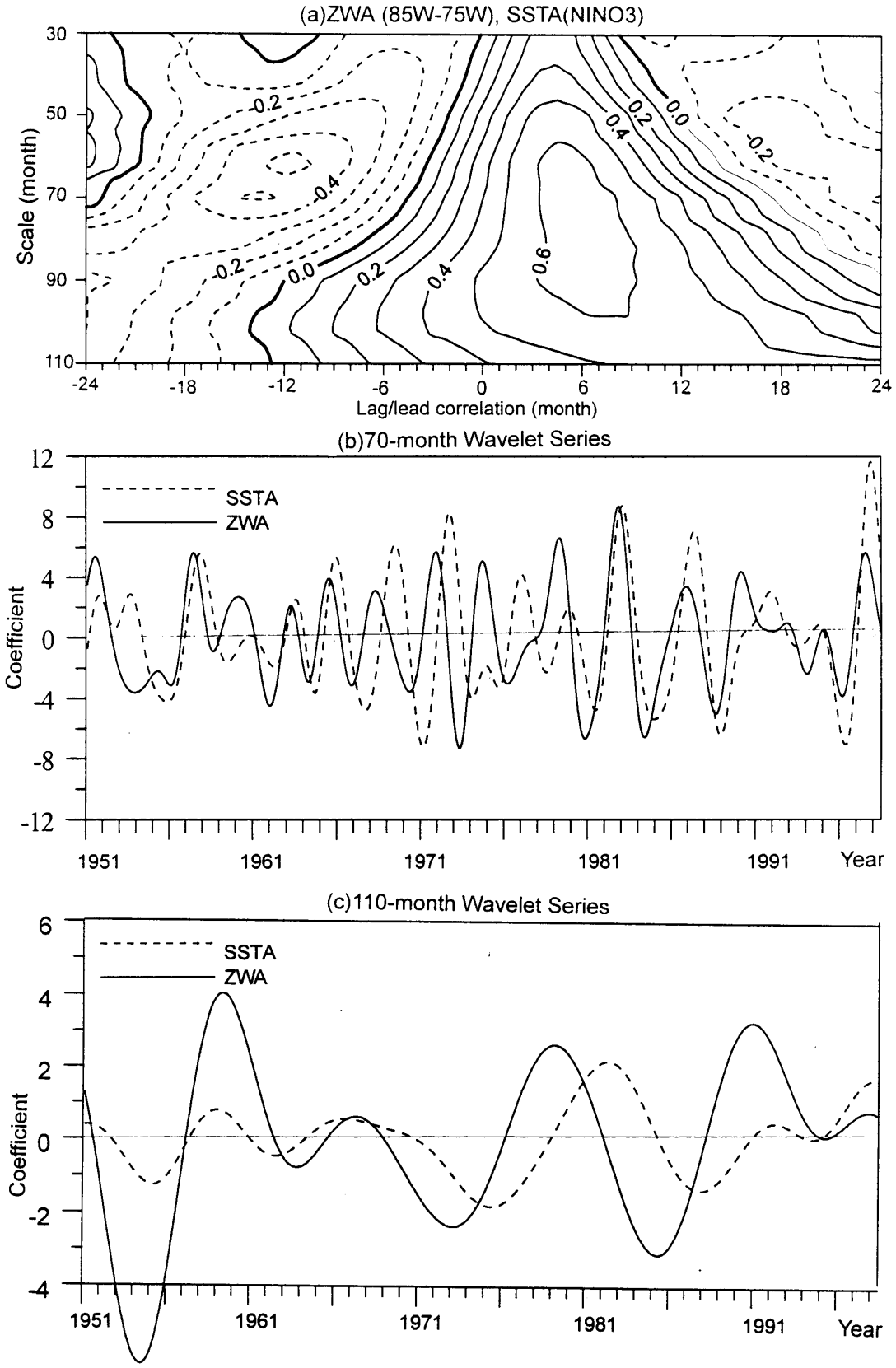

Fig. 6. Same as in Figure 4 but for ZWA at the region of 85W–75W in equatorial South American coast.

5. *Explanation for the relationship*

In our data handing, two processes, vertical integration and climatological mean departure, are performed. As well known standing Walker/Hadley circulation and moving local circulation cells exist in the tropical Pacific. The winds that are associated with the Walker circulation have opposite directions in the upper and lower levels so that the reflection of Walker circulation has been partly filtered out from the vertically-integrated values of zonal wind. After the performance, there should leave anomalous Hadley circulation and some anomalous local circulation with anomalous convergence and divergence patterns of zonal wind along the equatorial zone. These phenomena can be clearly seen from Figure 1, where the westerly anomaly and easterly anomaly along the whole equatorial zone associate with the anomalous Hadley circulation while the moving convergence/divergence is the local anomalies. Some local fluctuations originated from the equatorial western Pacific then shifted eastward. Obvious examples of these moving fluctuations are found in 1956–1959, 1975–79, 1988–89, 1991–92 and 1996–97.

Over the equatorial western Pacific and tropical eastern Indian Ocean, atmospheric convection is active due to the high SST and large water vapour content, particularly near the Inter-Tropical Convergence Zone (ITCZ), the place of the most frequent tropical deep convection. To explain the relationship between NINO3 region SSTA and ZWA at different regions in the Pacific Basin, a simple dynamical model, which is similar to previous studies (e.g., *Gill*, 1980; *Zebiak and Cane*, 1987; *Battisti et al*., 1999; and others), is applied. The governing dynamical equations describe a linear, steady state circulation with a tropospheric-scale vertical structure (*Zebiak*, 1986). On an equatorial, $\hat{A}$-plane the equations assume the following form:

$$\varepsilon u - \beta_0 yv = -\frac{\partial P}{\partial x}, \tag{2}$$

$$\varepsilon v + \beta_0 yu = -\frac{\partial P}{\partial y}, \tag{3}$$

$$\varepsilon P + C_a^2\left(\frac{\partial u}{\partial x} + \frac{\partial v}{\partial y}\right) = -Q, \tag{4}$$

where $P = p/\rho_0$; p, ρ_0 are the vertically-integrated air-pressure and density for tropical troposphere, respectively; $\beta_0 = 2\Omega/a$, Ω is angular velocity of the Earth's rotation and a the mean radius of Earth; u, v the vertically-integrated zonal and meridional wind anomalies; ε the damping coefficient; $C_a=(gH)^{1/2}$, g is the gravity acceleration, H is the depth of troposphere.

In Eq. (4), Q is the specified heating anomaly. According to *Zebiak* (1986), the heating anomaly was parameterized in terms of the local SSTA by considering tem-

perature-dependent changes in local evaporation. Linearizing the Clausius-Clapeyron relation about the mean sea surface temperature led to

$$Q = \alpha(SSTA)(b/T_m^2)\exp(-b/T_m) \tag{5}$$

where *SSTA* is the sea surface temperature anomaly, T_m is the specified mean sea surface temperature, and α and b are constants.

Considering only the terms dealing with heating and zonal wind anomaly, we deduce the vorticity equation and divergence equation as follows.

$$\varsigma \cong \frac{\beta_o y}{\varepsilon C_a^2} Q, \tag{6}$$

$$D = \frac{\beta_0 y}{\varepsilon}\varsigma - \frac{\beta_0}{\varepsilon}u \tag{7}$$

From Eq. (6), vorticity is zero along the equator because y=0. If the heating is located in the equatorial western Pacific, positive vorticity will appear in north of equator and negative in south of equator, so that anomalous westerly wind will develop along the equator, particularly to the west of warm center. On the other hand, from Eq. (7), convergence will be enhanced on the equator due to the development of westerly wind. The westerly wind anomaly in west of the warming center appears earlier than the peak of positive SSTA. According to local air-sea interaction, enhanced convergence will lead to enhanced heating from sea to air. Thus, Eqs. (6) and (7) describe a positive feedback process for this simple sea-air interaction system.

To see a negative feedback in the simple model, the model may be transformed into the zonal-mean one in the basin region as follows.

$$\varepsilon \overline{U} - \beta_0 y\overline{V} = 0, \tag{8}$$

$$\varepsilon \overline{V} + \beta_0 y \overline{U} = -\frac{\partial \overline{P}}{\partial y}, \tag{9}$$

$$\varepsilon \overline{P} + C_a^2 \frac{\partial \overline{V}}{\partial y} = -\overline{Q}\,. \tag{10}$$

From Eqs. (8–10), we may get the relationship between the zonal-mean heating anomaly and the zonal-mean ZWA as follows.

$$\overline{U} = \frac{\beta_0 y}{\varepsilon\left[\varepsilon^2 + (\beta_0 y)^2\right]} \cdot \frac{\partial \overline{Q}}{\partial y}. \tag{11}$$

It may be inferred from Eq. (11) that the zonal-mean ZWA always equals zero along the equator. During the phase of positive maximum SSTA over the equator, the zonal-mean easterly wind anomalies are located outside the equator because $y \cdot \frac{\partial \overline{Q}}{\partial y} < 0$ off the equator so that the easterly anomaly in the east part of the warming center is a negative feedback for the ENSO-like cycle. The negative feedback of SST rising along the coast, which needs to be explained by constructing a planetary scale air-sea system, is out of the scope in this paper.

6. Conclusion and discussion

The present paper analyzes the relationship between the NINO3 region SSTA and the tropospheric vertically-integrated ZWA at different regions over the Pacific Basin for a relatively long period from 1950 to 1998 using the homogeneous NCEP reanalysis data sets.

Wavelet analysis of both ZWA and SST anomaly shows that various phase-lag relationships exist in the interannual and interdecadal time-scales. In the equatorial western Pacific, the phase of ZWA precedes that of the EEP SST anomaly (or El Niño event) for about 7–13 months mostly at interannual timescale, which implies that westerly anomaly in western Pacific leads to SST rising in the EEP region. This relationship has been noted by previous studies but the preceding time is only one season and shorter than present finding with the tropospheric vertically-integrated ZWA. In the equatorial central Pacific, there is little phase-relationship between the local ZWA and NINO3 region SSTA. In the equatorial eastern Pacific, the phase of the EEP SST anomaly in most events is earlier than that of ZWA for about 4–9 months, which means that positive SSTA will lead to an easterly anomaly in the tropical eastern Pacific. The easterly anomaly in the tropical eastern Pacific may be the negative feedback of ENSO cycle. These relationships between the NINO3 region SSTA and ZWA at the equatorial western/eastern Pacific are in accordance with the tropical air-sea interaction scenario described by the Gill model.

In the equatorial South American coast, the phase of ZWA leads that of EEP SST anomaly about 6 months ahead at the interannual time scale, i.e., the El Niño event appears when the ZWA transforms from westerly to easterly while the La Niña event takes place in the reversed situation. This relationship is also seen from the decadal-scale variation of ZWA and SST anomaly near the coast. The relationship between NINO3 region SSTA and ZWA right at the coast has not been explained, though, because it requires consideration of air-sea interaction of multiple time-space scales as well as the atmosphere-earth angular momentum exchanges caused by mountain torques.

This paper suggests that ZWA at the equatorial western Pacific and South American coast can be used as an early signal for predicting the El Niño/La Niña events. Decade-scale active and break periods of tropical air-sea interaction have been observed,

which can probably account for the El Niño forecast deficiency during break period. And, the present active period, starting from 1996, is expected to have another two events in 2001/02 and 2005, in addition to the 1997/98 one.

Decade-scale active and break periods of tropical air-sea interaction may explain why the relatively lower skill levels of ENSO prediction existed in the early 1990s and mid 1970s relative to the 1980s. The new active period up to 2005 is good news for many models. In comparison with previous studies using surface winds, ZWA-SSTA relation becomes more evident because lag-time between them is longer and different phase-relationships in equatorial western, central, eastern Pacific and in the equatorial South America coast are found.

Acknowledgments

We extend our thanks to two anonymous reviewers whose comments and suggestions have improved the presentation of this paper. This research was supported by the National Key Program for Developing Basic Sciences in China (No. G1999043405) and the National Natural Foundation of China (No. 49975023). The first author would like to thank Professor S.-W. Wang for improving revised text.

Reference

Barnett, T.P., 1977. The principal time and space scales of the Pacific trade wind field, *J. Atmos. Sci.*, **34**, 221–235.

Barnett, T.P., 1983. Interaction of the monsoon and Pacific trade wind system at interannual time scales. Part I: the equatorial zone, *Mon. Wea. Rev.*, **111**, 756–773.

Barnett, T.P., M. Latif, N. Graham, M. Flügel, S. Pazan and W. White, 1993. ENSO and ENSO-related predictability. Part I: Prediction of equatorial Pacific sea surface temperature with a hybrid coupled ocean-atmosphere model, *J. Climate*, **6**, 1545–1566.

Barnston, A.G. and C.F. Ropelewski, 1992. Prediction of ENSO episodes using canonical correlation analysis, *J. Climate*, **5,** 1316–1345.

Battisti, D.S., E.S. Sarachik and A.C. Hirst, 1999. A consistent model for the larger-scale steady surface atmospheric circulation in the tropics, *J. Climate*, **12**, 2956–2964.

Chen, D., S.E. Zebiak, A.J. Busalacchi and M.A. Cane, 1995. An improved procedure for El Niño forecasting: Implications for predictability, *Science*, **269**, 1699–1702.

Dickey, J.O., S.L. Marcus and R. Hide, 1992. Global propagation of interannual fluctuations in atmospheric angular momentum, *Nature*, **357**, 484–488.

Gill, A.E., 1980. Some simple solutions for heat induced tropical circulation, *Q. J. Roy. Meteorol. Soc.*, **106**, 447–462.

Hickey, B., 1975. Relationship between fluctuations and sea level wind stress and sea surface temperature in the equatorial Pacific, *J. Phys. Oceanogr.*, **5**, 460–475.

Ji, M., A. Leetmaa and V.E. Kousky, 1996. Coupled model predictions of ENSO during the 1980s and the 1990s at the National Centers for Environmental Prediction, *J. Climate*, **9**, 3105–3120.

Latif, M., D. Anderson, T. Barnett, M. Cane, R. Kleeman, A. Leetmaa, J. O'Brien, A. Rosati and E. Schneider, 1998. A review of the predictability and prediction of ENSO, *J. Geophys. Res*. **103**, 14375–14393.

Latif, M., T.P. Barnett, M.A. Cane, M. Flugel, N.E. Graham, H.V. Storch, J.-S. Xu and S.E. Zebiak, 1994. A review of ENSO prediction studies, *Climate Dynamics*, **9**, 167–179.

Lau, K.-M. and H.-Y. Weng, 1995. Climate signal detection using wavelet transform: how to make a time series sing, *Bulletin of the American Meteor. Soc.*, **76**, 2391–2402.

Philander, S.G.H., 1983. El Niño Southern Oscillation phenomena, *Nature*, **302**, 296–301.

Philander, S.G.H., 1990. *El Niño, La Niña, and the Southern Oscillation*, 293 pp., Academic Press, San Diego.

Phillip, A.A., 1982. The relationship between interannual variability in the 200mb tropical wind field and the Southern Oscillation, *Mon. Wea. Rev*., **110**, 1393–1404.

Qian, W.-H., Y.-F. Zhu and Q. Ye, 1999. Interannual and interdecadal variability in SST anomaly over the eastern equatorial Pacific, *Chinese Science Bulletin*, **44**, 568–571.

Rasmusson, E.M. and T.H. Carpenter, 1982. Variations in tropical sea surface temperature and surface wind field associated with the Southern Oscillation/El Niño, *Mon. Wea. Rev*., **110**, 354–384.

Trenberth, K.E., 1997. The definition of El Niño, *Bulletin of the Amer. Meteor. Soc.*, **78**, 2771–2777.

Trenberth, K.E., 1998. Development and Forecasts of the 1997–98 El Niño: CLIVAR Scientific Issues, *Seventh session of the CLIVAR SSG in Santiago*, Chile (April 1998).

Wang, B., 1995. Interdecadal changes in El Niño onset in the last four decades, *J. Climate*, **8**, 267–285.

Zebiak, S.E., 1986. Atmospheric convergence feedback in a simple model for El Niño, *Mon. Wea. Rev.*, **114**, 1263–1271.

Zebiak, S.E. and M.A. Cane, 1987. A model El Niño-Southern Oscillation, *Mon. Wea. Rev.*, **115**, 2262–2278.

Zhu, Y.-F., W.H. Qian and Q. Ye, 1999. Tropical sea surface temperature anomaly and Indian summer monsoon, *Acta Meteorologica Sinica*, **13**, 154–163.